ARCHIVES OF ELECTRICAL ENGINEERING VOL. 61(4), pp. 471-482 (2012)

DOI 10.2478/v10171-012-0047-6

Analysis of permanent magnet linear motor parameters taking its heating into account

ANDRZEJ WAINDOK

Faculty of Electrical Engineering, Automatic Control and Informatics
Opole University of Technology
Prószkowska 76, 45-758 Opole

e-mail: a.waindok@po.opole.pl

(Received: 26.01.2012, revised: 21.03.2012)

Abstract: The calculation results of the static field parameters for permanent magnet linear synchronous motor have been presented in this work. The influence of the construction temperature on the parameters has been analyzed mathematically. Models for magnetic and temperature fields determination have been formulated. Two kinds of permanent magnets (NdFeB and SmCo) have been considered. The distribution of the thermal field has been obtained using the finite element method (FEM).

Key words: linear synchronous motors, thermal field calculation, permanent magnets parameters

1. Introduction

The rare earth permanent magnets (PMs) are used more and more frequently in the electrical machines and in linear actuators and motors, as well [2, 8]. The magnets with remanent magnetic flux density of $B_r = 1.4$ T and with coercive field strength value of $H_c = 1$ MA/m are used for construction of actuators with high force density i.e. force per unit mass of the mover, giving good dynamic properties [9]. The most popular PMs are NdFeB and SmCo. SmCo PMs have relatively low magnetic energy densities compared to the NdFeB PMs. Their advantage is high stability of parameters under temperature rising [2].

The parameters of PMs depend on temperature [3, 6]. Thus, it is important to determine, how the heating influences the electromagnetic parameters of the actuator. It is even more important in modern rotary and linear permanent magnet machines in which the high value of current density is forced. To maximize the windings exploitation, we need to assume a high current density value (sometimes 8-10 A/mm^2). The high density values lead to rapid heating of the windings, and consequently to heating of the whole construction, including build in permanent magnets. Thus, it is important to calculate the steady-state temperature in the machine parts after heating, caused by the long-time operation.

In the presented work, the analysis of the heating influence on the linear motor parameters has been studied. The calculations have been carried out for two kinds of PMs (NdFeB and SmCo) and for two different operating temperatures. In the first case the room temperature has been assumed, and in the second one the nominal steady-state temperature (for nominal current) has been assumed.

2. Physical model of the investigated linear motor

The investigated linear synchronous motor is a five-phase construction with permanent magnets [2, 7, 13]. The picture of the motor prototype has been presented in Figure 1. Cross section with main motor elements is visible in Figure 2 and 3.

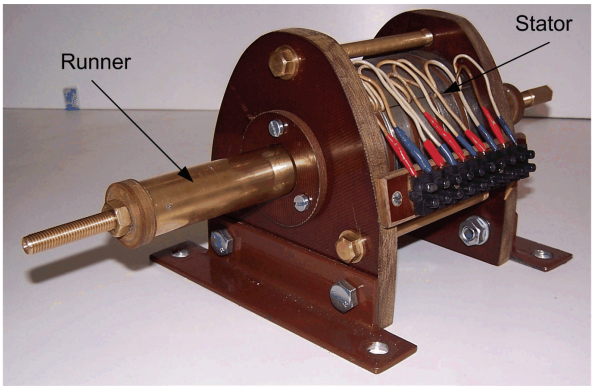

Fig. 1. Picture of the investigated linear motor

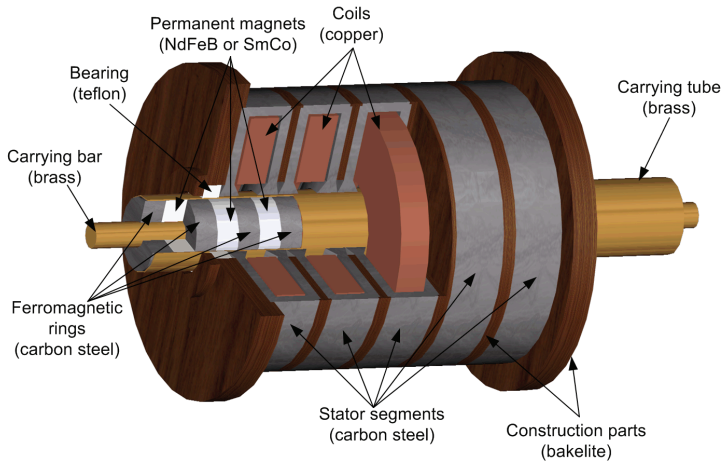

Fig. 2. Cross-section of the motor with major elements

It is an interesting solution compared to the 3-phase motors. The 5-phase motor is characterized by lower force ripples and lower detent force compared to the 3-phase construction. In the Table 1 the most important parameters of the motor have been given.

During the operation the temperature in the motor is arising from the excited current. In the positioning mode (current vector controlling) the current flows permanently. Thus, the controller influences the current intensity and this way forces the temperature of the machine.

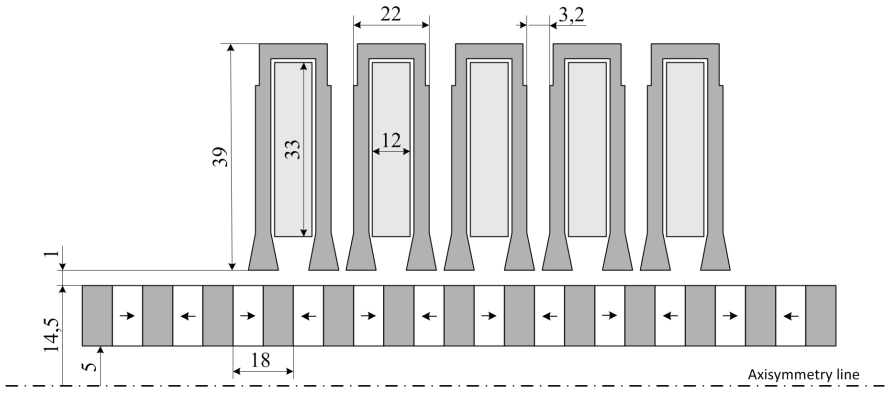

Fig. 3. Dimensions of the linear motor

Table 1. Most important parameters of the linear motor

Parameter	Quantity	Value
Maximum force	[N]	600
Nominal current (continuous work)	[A]	2.7
Maximum current	[A]	8
Nominal velocity	[m/s]	1
Nominal acceleration	[m/s^2]	100
Stroke	[m]	0.2

3. Mathematical model

In the paper, the overworked mathematical model, for the analysis of the magnetostatic field, has been used [10, 11]. Additionally, the new thermal model, created by the author, has been implemented. In the first step the temperature field has been determined with using the thermal model. Knowing the permanent magnet temperature, the linear motor parameters have been determined, respectively. The integral parameters of the field in the actuator (force and flux) have been calculated.

A) Thermal model

The static temperature field could be obtained after Poisson equation solution. The elliptic equation is expressed as [4]

$$\nabla \cdot (\kappa \nabla T) = -p, \tag{1}$$

where: p – power density generated in the unit volume [W/m^3], κ – thermal conductivity coefficient [W/(m · K)] (in the case of anisotropic medium it is a tensor quantity), T – temperature [K].

Taking into account the cylindrical symmetry of the analyzed motor, the equation (1) can be expressed as

$$\frac{1}{r}\frac{\partial}{\partial r}\left(r\kappa\frac{\partial T}{\partial r}\right)+\frac{\partial}{\partial z}\left(\kappa\frac{\partial T}{\partial z}\right)=-p. \tag{2}$$

Two different kinds of boundary conditions have been assumed for the 2D thermal problem. The first one is a Dirichlet condition, which allows us to assume the fixed temperature value T_0 on the outer boundary of the calculation region. The second one is the boundary condition for the convection. The heat transfer through the outer surface of the motor is expressed as

$$\kappa \nabla T \cdot \vec{n} + h(T - T_0) = 0, \tag{3}$$

where h – heat transfer coefficient [W/(m^2 · K)], $\vec{n}$ – unit vector normal to the boundary surface of the machine.

In the thermal analysis the radiation phenomenon has been neglected. It is due to relatively low temperature of the machine outer surface.

B) Magnetostatic model

As the analyzed motor is characterized by the cylindrical symmetry, the partial differential equation for the modified magnetic vector potential $(A'_\varphi = rA_\varphi)$ can be expressed as [1]:

$$\frac{\partial}{\partial r}\left(\frac{1}{r\mu(B)}\frac{\partial A'_\varphi}{\partial r}\right)+\frac{\partial}{\partial z}\left(\frac{1}{r\mu(B)}\frac{\partial A'_\varphi}{\partial z}\right)=-J_\varphi. \tag{4}$$

After solving the equation above, the potential value is obtained and is used for magnetic flux density calculation and for determining the magnetic flux linked with the windings [1, 12]:

$$\vec{B} = -\frac{1}{r}\frac{\partial A'_\varphi}{\partial z}\vec{1}_r + \frac{1}{r}\frac{\partial A'_\varphi}{\partial r}\vec{1}_z, \tag{5}$$

$$\Psi = \sum_{k=1}^{N}\int_S B_n \mathrm{d}S = \sum_{k=1}^{N}\int_l A_t \mathrm{d}l, \tag{6}$$

Using the parameters above, the dynamic inductance and electromagnetic force acting on the runner can be determined [11]:

$$L_{\mathrm{d}} = \frac{\partial \Psi}{\partial i}, \tag{7}$$

$$\vec{F}_e = \frac{1}{2}\oint_{\Gamma}\left(\vec{H}\left(\vec{B}\cdot\vec{n}\right)+\vec{B}\left(\vec{H}\cdot\vec{n}\right)-\left(\vec{H}\cdot\vec{B}\right)\vec{n}\right)\mathrm{d}\Gamma. \tag{8}$$

4. Calculation results

In the Table 2 the permanent magnet parameters are given. The conductivity constants for various materials are given in Table 3.

Table 2. Permanent magnet parameters [14, 15]

Parameter	Quantity	NdFeB	SmCo
B_{r}	[T]	1.25	1.01
H_{c}	[kA/m]	950	724
$\boldsymbol{\mu_{\mathrm{r}}}$	–	1.048	1.11
T_{c}	[°C]	300	850
Working temperature	[°C]	80	300
$(BH)_{\max}$	[kJ/m^3]	310	203
Temperature coefficient for B_{r}	[%/°C]	–0.11	–0.04
Temperature coefficient for H_{c}	[%/°C]	–0.5	–0.27

Table 3. Thermal conductivity of materials assumed in the thermal model [5, 15]

Material	κ [W/(m · K)]
Copper	401
Bras	110
Steel	54
Teflon	0.35
Air	0.031
NdFeB	7.7
SmCo	9.3
Bakelite	0.23

First, the calculations have been carried out for determining the permissible power density losses, which does not cause the overheating of the permanent magnets. The ambient temperature has been assumed to be equal T_0 =20°C (293°K). The highest temperature for wire isolation is T = 180°C (453°K). The heat transfer coefficient has been assumed to be constant at all outer motor surfaces and equal to h = 11 W/(m^2 · K). Its value has been determined on the basis of heating measurements. It is very difficult to obtain it computationally, because the

mathematical model of fluid flow has to be solved, which is more difficult, than the problem presented in the paper.

The temperature fields obtained for the permissible power density losses are presented in Figures 4 and 5. For the linear motor with NdFeB magnets the temperature field is presented in Figure 4. For the motor with SmCo PMs the field is given in Figure 5. The power density values of the heat source have been determined iteratively. The temperatures of PM's and windings have been determined in each iteration. The calculations have been interrupted, when the upper limit of the temperature for the constructional parts had been achieved (Table 2). In the case of motor with NdFeB magnets the P/V = 200000 W/m^3 value has been obtained, and in the case of motor with SmCo P/V = 283000 W/m^3 (Table 5). The motor with SmCo magnets is characterized by higher power density value due to higher limit working temperature of the magnets.

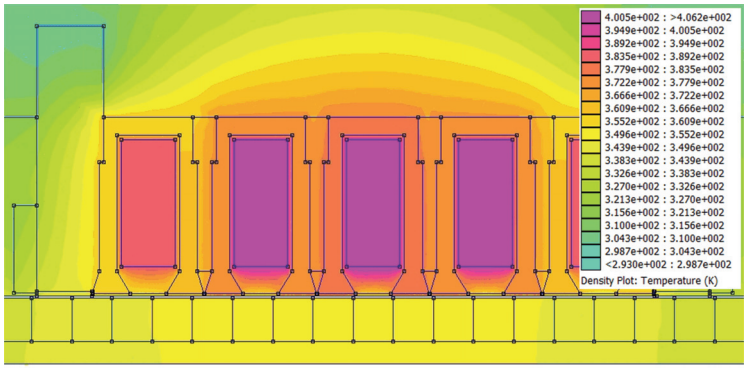

Fig. 4. Temperature field distribution for a motor with NdFeB PMs, P/V = 200000 W/m^3

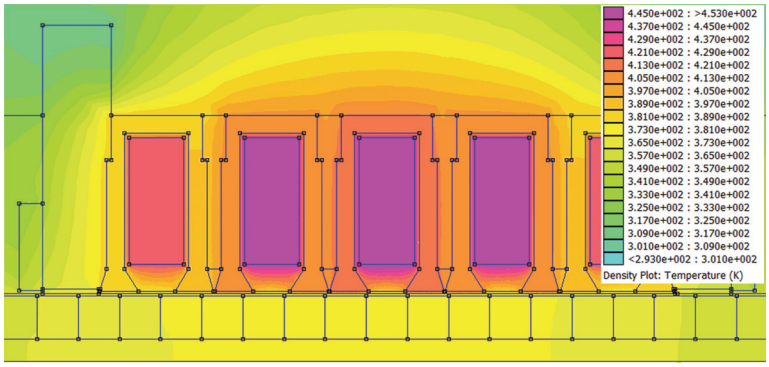

Fig. 5. Temperature field distribution for a motor with SmCo PMs, P/V = 283000 W/m^3

Knowing the values of the maximal power density losses in the windings (for continuous work), it is possible to calculate the magnetic force and flux. The force characteristic versus runner positions, has been obtained for nominal load angle value. The flux characteristic verso excitation current has been determined for phase no 3 and for neutral position of the runner [2, 13].

Before the magnetostatic calculations are carried out, the parameters of the permanent magnets and values of the excitation currents, for given operating temperature, have to be determined. The remanent magnetic flux density and coercive field strength values are obtained from the equations (temperature T is given in Kelvins) [2].

$$B_{\mathrm{r}} = B_{\mathrm{r}20}\left[1 + \frac{\delta B_{\mathrm{r}\%}}{100}(T - 293)\right], \tag{9}$$

$$H_{\mathrm{c}} = H_{\mathrm{c}20}\left[1 + \frac{\delta H_{\mathrm{c}\%}}{100}(T - 293)\right]. \tag{10}$$

The symbols $\delta B_{\mathrm{r}\%}$ i $\delta H_{\mathrm{C}\%}$ denotes the temperature coefficients for the remanent magnetic flux density and coercivity, respectively. Including the appropriate parameters in equations (9) and (10), the values of remanent magnetic flux density and coercive field strength, for the considered PM temperature (Table 4), could be obtained. The temperature values in Table 4 have been obtained from the numerical calculations. The maximum working temperature of NdFeB has been assumed to be 353 K, and the maximum operation temperature for SmCo has been assumed to be 573 K (Table 2). The highest operation temperature for SmCo is much higher than the limit temperature of the winding insulation (453 K). Thus, the temperature in SmCo has been calculated assuming the limit winding temperature to be equal 453 K.

The value of the excitation current depends on the temperature of motor operation. It is due to the variable value of the electric resistance, which is changing according the temperature. Keeping the current constant the power losses increase. Thus, to keep the power losses density to be constant, the excitation current should be changed. In Table 5 the current values for different winding temperatures and constant power losses densities are given. In the room temperature, the resistance of a single coil in the considered motor is R = 1.42 Ω. To determine the resistance in a higher temperature the known equation has been used:

$$R = R_{20}\left[1 + \alpha(T - 293)\right]. \tag{11}$$

For copper wires the coefficient is α = 0.0039 1/K. The calculation results are shown in Figures 6 to 11.

Table 4. Permanent magnet parameters in higher temperatures

Material	T [K]	B_{r} [T]	H_{c} [kA/m]	μ_{r}
NdFeB	353	1.168	665	1.398
SmCo	378	0.976	558	1.392

Table 5. The excitation current values for different winding temperature and constant power losses density

PM material	Power density [W/m^3]	Winding temperature T [K]	R [Ω]	I [A]
NdFeB	200000	293	1.42	3.25
		406	2.046	2.71
SmCo	283000	293	1.42	3.86
		453	2.306	3.03

Taking into account the main factors, which occur during the continuous operation of the motor, i.e. the permissible working temperature of the permanent magnets and windings and the variations of the permanent magnet parameters and winding resistance, it comes out, that there is no significant difference between parameters of the motor assembled with using the NdFeB or SmCo. Despite the fact the SmCo PMs are characterized by much higher working temperature, and thus it is possible to increase the excitation current density, the parameters of the motor are worse than the parameters of the motor build with using the NdFeB magnets. The force values are slightly higher (approximately 5-6%) for the motor with NdFeB magnets (Figure 6). With the increasing of the temperature to the permissible value, the average force value decreases in both cases by 36-38 %.

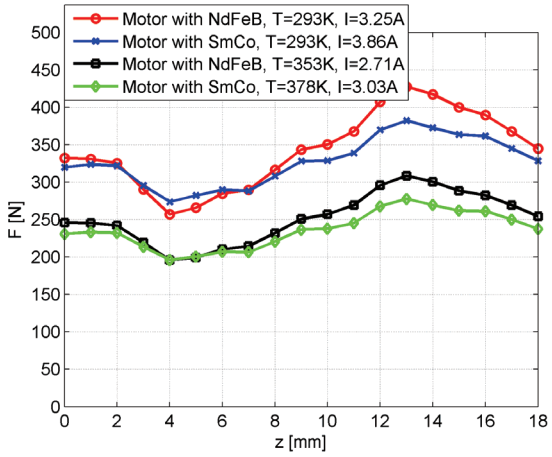

Fig. 6. Force value versus runner position for nominal load angle and constant power density

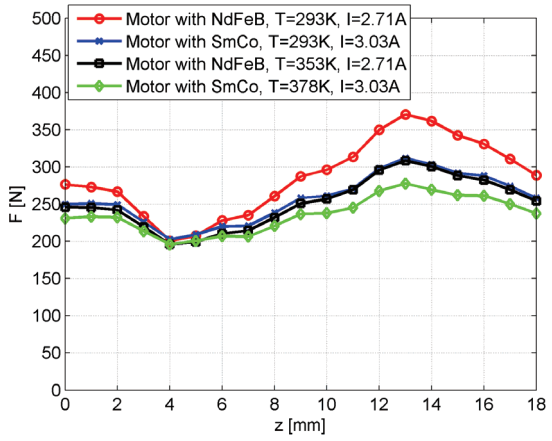

Fig. 7. Force value versus runner position for nominal load angle and for nominal current

The analysis for constant power density, which is described above, is not very accurate. In the real systems either current or voltage values are constant. In the case of constant voltage value the power is decreasing during the winding heating. In the case of constant current value, the power increases with the winding temperature. For the PWM supplying, we can assume that the current level is constant. In such a case, the nominal current value for cold and hot motor has to be the same. It means, that in the magnetostatic model we have to assume the lower values of the excitation current, obtained for the higher temperature (Table 5). It is $I = 2.71$ A for the motor with NdFeB magnets and $I = 3.03$ A for the motor with SmCo magnets. The calculation results of the force characteristic are presented in Figure 7. The differences between cold and hot motor are lower, than in Figure 6. In the case of a motor with NdFeB the force decreases about 14% after heating the motor, whereas in the case of SmCo magnets the force decreases about 8.5%.

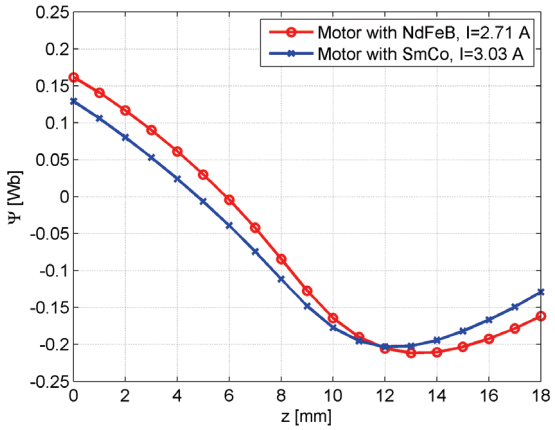

Fig. 8. Motor flux linkage versus runner position for phase no 3 and for neutral position of the runner ($T = 20$°C)

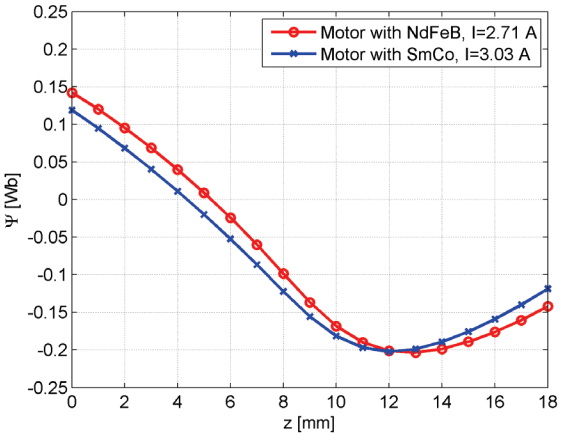

Fig. 9. Motor flux linkage versus runner position for phase no 3, for neutral position of the runner and for higher temperature (Tables 4 and 5)

In both, low and high motor temperature, the force for a motor with NdFeB is higher compared to the force for a motor with SmCo (12% for cold motors and 6% after heating).

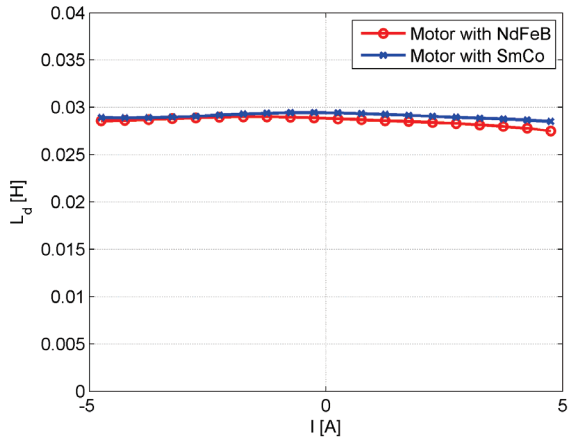

Fig. 10. Dynamic inductance versus current value for phase no 3 and for neutral position of the runner ($T = 20°C$)

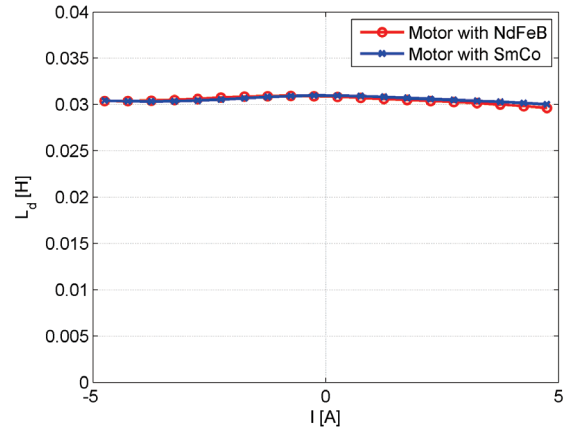

Fig. 11. Dynamic inductance versus current value for phase no 3 and for neutral position of the runner for higher temperature (Tables 4 and 5)

In the case of the magnetic flux coupled with the winding, the magnet material influences the values of the flux only slightly (Fig. 8). Increasing the temperature, decreases slightly the value of the magnetic flux (Fig. 9). It is due to the decreasing of the permanent magnet energy in higher temperature. The same is observed in the case of dynamic inductance values (Figs. 10 and 11), which almost do not depend on the PM material. The L_d parameter values increases slightly after motor heating (Fig. 11).

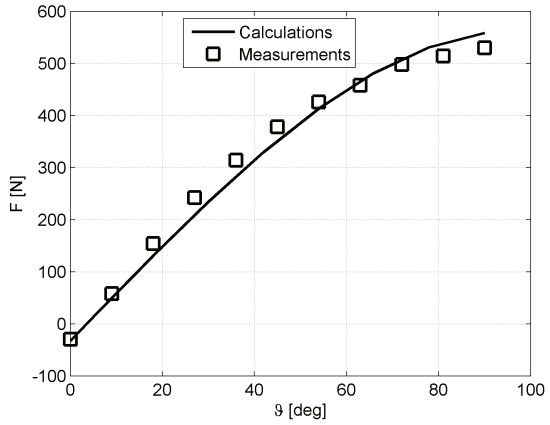

Fig. 12. Measurement verification of the force characteristic versus load angle for room temperature

In Figure 12 the measurement verification for the prototype assembled with using the NdFeB PMs has been given additionally. During the experimental test the PM temperature was close to the room temperature. There is a good conformity between measurement and calculation results visible, which confirms the correctness of the numerical model of the investigated linear motor.

5. Conclusions

The electromagnetic parameters of linear motors assembled using two different kinds of permanent magnets (NdFeB and SmCo) have been compared. The heating of the windings and the influence of the temperature on the permanent magnets and the motor static parameters have been taken into account in the calculations. According the calculation results, the differences between parameters of the motor with NdFeB or SmCo magnets are very small. The motor with NdFeB has slightly better parameters, than the one with SmCo magnets.

If the working temperature does not exceed the allowed values for the NdFeB magnets, it is more convenient to use them instead of SmCo magnets.

References

[1] Bolkowski S., Stabrowski M., Skoczylas J. et al., *Komputerowe metody analizy pola elektromagnetycznego*. (*Computer methods for electromagnetic field analysis*), (in Polish). WNT, Warszawa (1993),

[2] Gieras J.F., Piech Z.J., Tomczuk B., *Linear synchronous motors.* CRC Press, Taylor & Francis Group, USA (2011).

[3] Haavisto M., Paju M., *Temperature stability and flux losses over time in sintered Nd-Fe-B permanent magnets.* IEEE Trans. on Magnetics 45(12): 5277-5280 (2009).

[4] Kącki E., *Równania różniczkowe cząstkowe w zagadnieniach fizyki i techniki.* (*Partial differential equations in the physic and technique problems*), (in Polish).WNT, Warszawa (1992).

[5] Lide D.R., *Handbook of chemistry and physics.* 84th Edition, CRC Press LLC (2004).
[6] Ruoho S., Haavisto M., Takala E. et al., *Temperature dependence of resistivity of sintered rare-earth permanent-magnet materials.* IEEE Trans. on Magnetics 46(1): 15-20 (2010).
[7] Tomczuk B., Waindok A., *A coupled field-circuit model of a 5-phase permanent magnet tubular linear motor.* Archives of Electrical Engineering 60(1): 5-14 (2011).
[8] Tomczuk B., Koteras D., Waindok A., Zimon J., *Polowa analiza siłowników elektromagnetycznych i transformatorów*. (*Field analysis of the electromagnetic actuators and transformers.*), (in Polish). Pomiary Automatyka Kontrola (PAK) 3: 264-268 (2011).
[9] Tomczuk B., Waindok A., *Linear motors in mechatronics – achievements and open problems*. *Monography: Transfer of innovation to the interdisciplinary teaching of mechatronics for the advanced technology needs.* Opole University of Technology, OWPO, pp. 343-360, Opole, Poland, (2009).
[10] Tomczuk B., Schröder G., Waindok A., *Finite element analysis of the magnetic field and electromechanical parameters calculation for a slotted permanent magnet tubular linear motor.* IEEE Trans. on Magnetics 43(7): 3229-3236, New York, USA (2007).
[11] Tomczuk B., Waindok A., *Integral parameters of the magnetic field in the permanent magnet linear motor. Monography: Intelligent Computer Techniques in Applied Electromagnetics* (in series *Studies in Computational Intelligence*), Springer Verlag 119: 277-281, Heidelberg, Germany (2008).
[12] Tomczuk B., Waindok A., Zimon J., *Polowe obliczanie parametrów elektromagnetycznych silników liniowych i łożysk magnetycznych.* (*Field calculation of electromagnetic parameters for linear motors and magnetic bearings.*), (in Polish). Przegląd Elektrotechniczny (Electrical Review) 85(3): 111-114 (2009).
[13] Waindok A., *Symulacja komputerowa i weryfikacja pomiarowa charakterystyk silnika liniowego tubowego z magnesami trwałymi.* (*Computer simulation and measurement verification of the permanent magnet tubular linear motor.*), (in Polish). Ph.D. thesis under Prof. B. Tomczuk supervision, Politechnika Opolska, Opole (2008).
[14] http://cibas.it/documents/SMCO.pdf – parameters of the SmCo magnets (12 March 2012).
[15] www.mmcmagnetics.com – parameters of the magnets (12 March 2012).